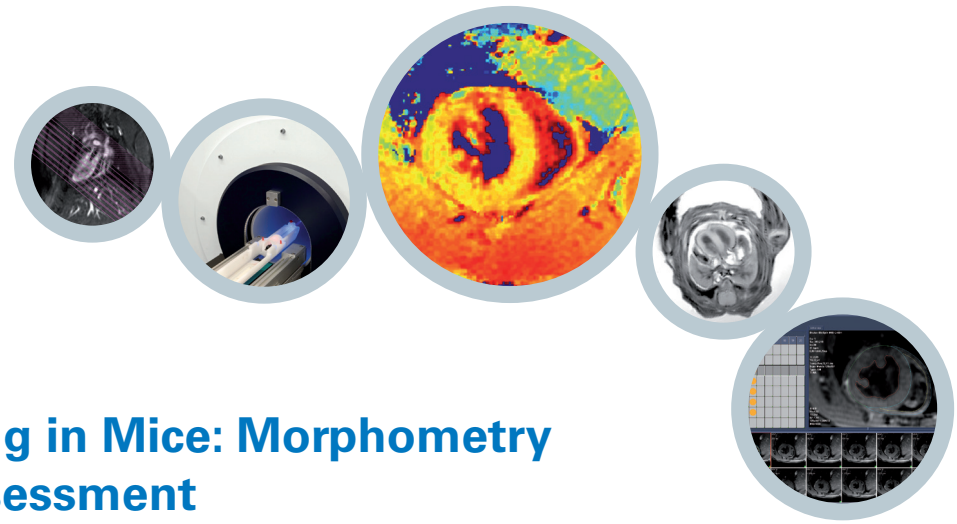

Cardiac MR Imaging in Mice: Morphometry and Functional Assessment

Andreas Pohlmann[1], Philipp Boyé[2], Babette Wagenhaus[1], Dominik Müller[2], Mateusz Kolanczyk[3], Sascha Köhler[4], Jeanette Schulz-Menger[2] and Thoralf Niendorf[1,2]

[1)] Berlin Ultrahigh Field Facility (B.U.F.F.), Max Delbrück Center for Molecular Medicine (MDC), Berlin, Germany,
[2)] Experimental and Clinical Research Center, Charité University Medicine, Campus Berlin-Buch, Germany,
[3)] Research Group Development and Disease, Max Planck Institute for Molecular Genetics, Berlin, Germany
[4)] Bruker BioSpin MRI GmbH, Ettlingen, Germany

Abstract

In cardiac MR imaging of mice a variety of different imaging techniques are available[1-2], ranging from morphometry, strain and velocity imaging, angiography, to perfusion and myocardial function, to name a few. In this report examples of cardiac MR imaging applications in mice are provided with a focus on morphometric and cardiac function assessment. Practical considerations for cardiac MR in mice are outlined and current trends - such as the trend towards self gating techniques - are surveyed.

Introduction

The art of producing animal models has significantly advanced over the past 15 years. Transgenic models have become common place in cardiac research. The crux of the matter still is adequate characterization and phenotyping of animal models to assure investigators that the appropriate conclusions can be drawn. Hence there is a need for non-invasive *in vivo* imaging (i) which provides superb spatial and temporal resolution for cardiovascular research, (ii) a high reproducibility and (iii) which is suitable for longitudinal studies. Realizing these challenges the use of MRI is conceptually appealing for the pursuit of cardiovascular research. The field of cardiovascular MR (CMR) has evolved rapidly over the past decade, feeding new applications across a broad spectrum of research areas. CMR applications include assessment of cardiac anatomy, regional wall motion, myocardial perfusion, myocardial viability plus cardiac chamber quantification and cardiac function assessment. Cardiac MR research includes assessment of myocardial infarction and myocardial injury, explorations into genetically or pharmacologically induced hypertension, characterization of progression and regression of exercise or pressure overload induced myocardial hypertrophy and identification of hormonal or sex specific effects of cardiac damage and cardiac (dys) function.

Functional Cardiac MR imaging

Dynamic imaging of the heart for the assessment of cardiac morphology, myocardial contractile function and wall motion requires high muscle/blood contrast, full coverage of the cardiac cycle and high temporal resolution. To balance these constraints gradient echo based CINE imaging techniques are used. Since cardiac MRI is not a real time imaging modality data acquisition is propagated over a series of heart beats which requires synchronization with the cardiac cycle. For this purpose ECG is commonly used for cardiac gating. ECG being an electrical measurement is disturbed by interference with the magnetic field, which is pronounced at ultra high fields such as 9.4 T. Hence, self gating techniques, such as IntraGate, are a very helpful alternative for robust cardiac imaging in mice and have been shown not to compromise the accuracy of the derived myocardial function parameters[3-4].

Experimental protocol

Because of the animal's small size and heart rates ranging between 400 and 600 beats per minute (bpm) tailored imaging protocols and dedicated cardiac hardware/software are essential to achieve appropriate temporal and spatial resolution for CMR in mice.

Hardware: Bruker Biospec 94/20. Bruker four-element cardiac coil array used for signal reception in conjunction with a Bruker linear volume resonator (ID 72 mm) used for signal transmission.

Imaging protocol and sequence parameters: Cardiac gating is a requirement for obtaining acceptable image quality. The IntraGateFLASH sequence allows retrospective gating and is recommended because it is non-invasive, more reliable, provides better signal-to-noise and contrast-to-noise[4] and more user friendly versus subcutaneous ECG needle electrodes. It is designed to reduce if not eliminate R-wave misregistration frequently encountered with ECG gating. In practice, IntraGate dramatically helps to reduce animal preparation time, especially in a high through-put setting. An expected heart rate and respiration rate (obtained from the physiological monitoring) are required by the IntraGateFLASH sequence a priori. The LV function assessment protocol comprises 4 sets of scans:

- **Scan 1)** Tri-pilot multi slice, ScanMode 'PilotScan', TR 85 ms, TE 1.5 ms, FOV 35 mm, 3x7 slices of 0.7 mm thickness, 10 repetitions.

- **Scan 2 & 3)** Single slice IntraGateFLASH cine, ScanMode 'RetrospectiveGating', TR 5 ms, TE 2.9 ms, FOV 35 mm, matrix size 128 zero-filled to 256, 0.7 mm thickness, 30 repetitions, 10 cardiac movie frames (cardiac phases).

- **Scan 4)** Multi slice IntraGateFLASH cine, TR 72 ms, TE 2.1 ms, FOV 30 mm, matrix size 192x128 zero-filled to 256, 8 slices of 0.8 mm thickness, 70 repetitions, 20 cardiac movie frames (cardiac phases), acquisition time 10 min 51 sec.

Anesthesia and physiological monitoring: 1.0-2.0% Isoflurane in an air/O_2 mixture with flow rates of 200 ml/min each. Respiration rate, body temperature, and heart rate (via pulse oximeter) are monitored using an MR compatible small animal monitoring and gating system (Model 1025, SA Instruments, Inc., Stony Brook, NY, USA). Animals are placed prone on the heart array coil and a stable body temperature is maintained by a warm water heating

Planning of standard cardiac views: There are three established standard views in cardiac MRI in mice: long axis two chamber view (2CV), long axis four chamber view (4CV), and short axis view (SAX). Due to the double oblique orientation of the heart, these views have to be achieved in several steps, starting with a multi-slice tri-pilot. After acquisition of the tri-pilot (scan 1), scan 2 needs to be planned on a coronal view so that the slice connects the apex and the center of the left atrioventricular valve (mitral valve) as illustrated in Figure 1 (left). For the next scan (scan 3) slice positioning is done in the same manner but perpendicular to the reference scan 2, as demonstrated in Figure 1 (center). Finally, the SAX slice package is positioned perpendicular to the reference scan 3 as well as perpendicular to the long heart axis. Cardiac chamber quantification and quantitative LV function assessment require the slice package to cover the entire left ventricle from the apex to the mitral valve for all cardiac phases. The first slice should be positioned just below the mitral valve in end diastole. The last slice should not show any lumen any more. Blood suppression for a better blood/endocardium contrast is achieved by placing a saturation band over the atria parallel to the imaging slice package with a gap of approximately one slice thickness. The slice thickness of the saturation slice must be wide enough to cover the atria and afferent vessels (*venae cavae* and pulmonary vein) as shown in Figure 1 (right).

Figure 1

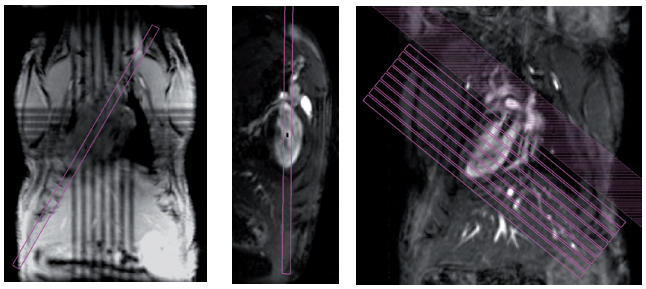

Fig. 1: Planning the geometry of a short axis (SAX) slice package, shown are scans 1, 2 and 3.

Subsequently, the 2CV and 4CV views can be planned on the SAX view by rotating a perpendicular slice so that it runs through the center of the left ventricle and, in the case of the 4CV, also through the right ventricle at it largest extend; the 2CV would not cross the right ventricle, but be rotated by 90°, i.e. perpendicular to both, the SAX and 4CV views.

Image analysis: Contrary to the perhaps common notion that left ventricular assessment using image segmentation is just drawing a few circles around the myocardium, first class data analysis is of key importance for LV function assessment to make sure that the mean inter-observer variability is below 5%. Hence careful segmentation of epi- and endocardial borders (Figure 2) is required. To achieve this goal by manual segmentation the use of commercially available software (for example Mass4Mice, Medis, Leiden, The Netherlands in our case) is advised. Alternatively, automated segmentation approaches may help to reduce the bias of intra- and inter-.observer variability[5-6]. Epi- and endocardial borders are segmented for all slices covering the left ventricle for cardiac phases derived from end systole and end diastole as depicted in Figure 3. The results obtained include the end systolic volume (LVESV) in ml, the end diastolic volume (LVEDV) in ml, the left ventricular ejection fraction (LVEF) in percent, the stroke volume in ml, and the ventricular mass (LVM).

Figure 2

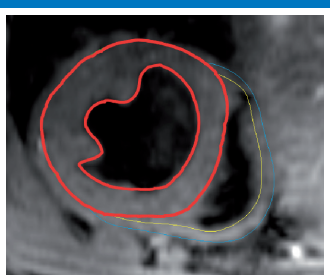

Fig. 2: Analysis of short axis slice package. Manual segmentation of the left and right ventricles.

Quantitative analysis of the right ventricle is also possible but challenging because it is rather thin and sometimes difficult to delineate against surrounding tissue. Ideally, both, left and right ventricle, should be captured in separate scans. Two separate scans allow for an optimized positioning of the flow saturation bands and whole coverage of the RV. Here multi-oblique orientation of the saturation slice with respect to the imaging slices would help to further improve blood saturation.

Figure 3

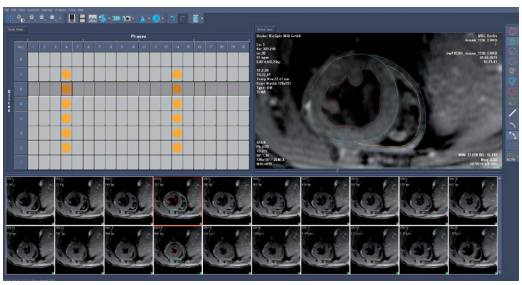

Fig. 3: Survey of whole heart 2D CINE short axis views of a mouse heart obtained at 9.4 T and basic overview of its use for LV function assessment and cardiac chamber quantification. For LV function assessment LV endo- and epicardial contours were manually traced for each slice for end-diastolic and end-systolic images.

Results and Discussion

Short axis (SAX) views comprising an end diastolic phase with apex-to-base coverage of a healthy mouse are shown in Figure 4. Blood typically white in FLASH sequences is suppressed by the regional flow saturation band and hence appears black (black blood technique). This approach helps to avoid flow artefacts and affords enhanced blood/myocardium contrast which supports the delineation of the myocardium

Figure 4

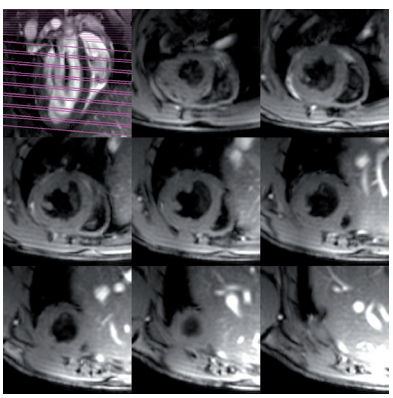

Fig. 4: SAX view of a healthy mouse heart at end diastole. Top left: geometry of SAX slices and flow saturation band. Top center to bottom right: eight SAX slices going from below the atria down to the apex.

Figure 5 shows a comparison of SAX views derived from a healthy mouse heart (left) with images obtained from animal models of myocardial infarction (middle and right) For this purpose occlusion of the left anterior descending LAD coronary artery was applied. Significant wall thinning can be observed for the segments in the anterior (center) and lateral (right) wall.

Figure 5

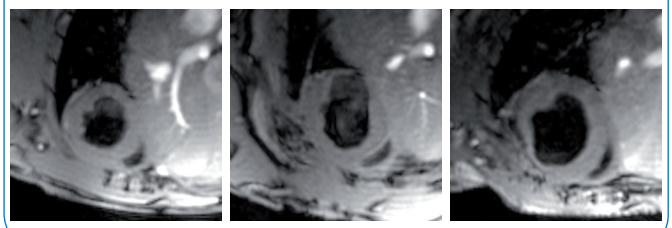

Fig. 5: SAX views of a healthy mouse heart (left) and hearts four weeks after a myocardial infarction (center and right), shown in diastole.

Figure 6 shows a four chamber view (4CV) of a healthy mouse heart (left) and a heart four weeks after a myocardial infarction (LAD occlusion) in diastole. The left ventricle is markedly enlarged and the apical segments of the myocardium are reduced to a very thin layer. In this case no extra blood suppression was applied.

Figure 6

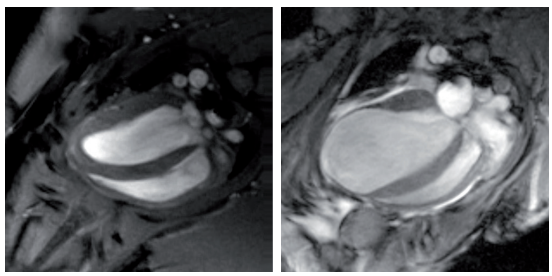

Fig. 6: Four chamber views (4CV) of a healthy mouse heart (left) and a heart four weeks after a myocardial infarction (right), shown in diastole.

Practical remarks: While gross effects of myocardial infarction, such as those shown in Figures 5 and 6, can easily be visually assessed in the SAX and 4CV views, this does not provide any quantitative information about the underlying pathology, which is essential in most studies. More subtle pathologies may also remain undetected. The quantitative analysis allows group statistics and calculation of significance levels. While severe myocardial infarction will inevitably lead to an impaired function and hence a reduced ejection fraction (EF), hypertension may induce hyperthrophy and hence result in an increased left ventricular mass. The sum of both ventricular masses should ideally add up to the actual heart weight obtained from post mortem quantification. Here extra caution should be taken since this correlation depends on the density of myocardial tissue which is used in the data analysis software to derive the ventricular mass from the volume of the myocardium. Other possible reasons for discrepancies are systematic errors during segmentation as well as suboptimal slice positioning or imperfect heart coverage. While the *in vivo* MRI derived absolute heart mass may deviate from ex vivo quantification we do want to emphasize linear regression of R>0.94 between both methods. Also, relative changes are a valuable measure for rapid phenotyping or of pathology in longitudinal studies and group studies with a matched control group. For example, Figure 7 shows EF and LVEDV differences in mice after myocardial infarction compared to a control group.

Figure 7

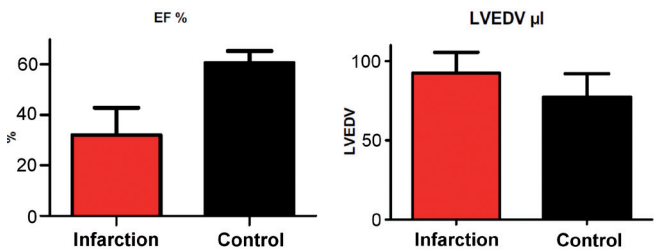

Fig. 7: Comparison of mice after infarction with control animals (n=8). Parameters derived from cardiac chamber quantification using CMR. Significant differences occurred in the EF (left, reduced after infaction, $p < 0.0001$) and LVEDV (right, increased after infaction, $p < 0.05$).

Pre-histological screening of mice embryos by ex vivo cardiac MRI

Congenital abnormalities in genetically modified mice may be detected already in embryos. 3D ultra high resolution ex-vivo MRI can depict the immature heart in sufficient detail for the assessment of morphological abnormalities[7]. Figure 8 shows an axial slice of mouse embryos, fixed in contrast agent and embedded in agarose. The overnight scan was performed using a quadrature mouse volume coil (ID 35mm) and a 600x512x512 acquisition matrix resulting an isotropic spatial resolution of 53 micrometer. While the use of the Bruker CryoCoil would allow for an even higher spatial resolution, the room temperature mouse volume coil allows screening a large number of animals simultaneously in a reasonable time. Based on this data histological analysis may be limited to a subset, i.e. only a manageable number of selected animals.

Figure 8

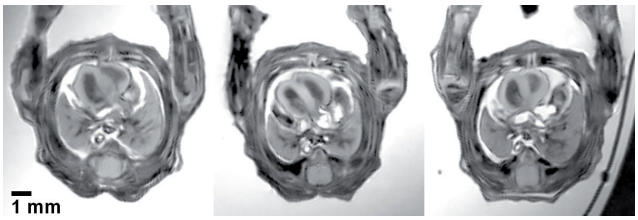

Fig. 8: µMRI with an isotropic resolution of 53 um, which allows the assessment of heart morphology in mouse embryos. The diameter of the hearts shown in these images is merely approx. 2 mm.

Parametric tissue mapping

CMR is also in the spotlight for monitoring non-invasively myocardial injury on a tissue level using quantification of MR signal changes and parametric mapping, which provides quantitative data as shown for a normal mice in Figure 9. For example the loss of structural homogeneity of the myocardium in favor of fibrotic tissue or collagen is assumed to induce changes in the native T_1, times of myocardium but also in the T_2 relaxation times. Admittedly, the high heart rate in small rodents renders accurate T_1 mapping challenging. Commonly used techniques such as Look-Locker (in our case Bruker trigFisp) provide good image quality and more than sufficient time points for T_1-mapping within a reasonable acquisition time[8]. It should be noted that this technique does not provide the true T_1 values of the tissue, but T_1*, which depends on the effective equilibrium longitudinal magnetization and hence on the acquisition parameters. The approach used in current research practice samples multiple time points along the T_1 recovery using a fixed sampling interval assuming constant heart rates or fixed R-R interval length for T_1-quantification. This can be an issue since variable heart rates during imaging cause data to be acquired at inconsistent time points of the T_1 recovery introducing a significant source of error in measured T_1 values. This is pronounced for imaging of mice models, where T_1 relaxation times of myocardium are significantly longer than several R-R intervals. These problems can be addressed by dynamic triggering (excitation loop running without acquiring data while waiting for the next R-wave) and retrospective assignment of MR data to the T_1-recovery curve

Figure 9

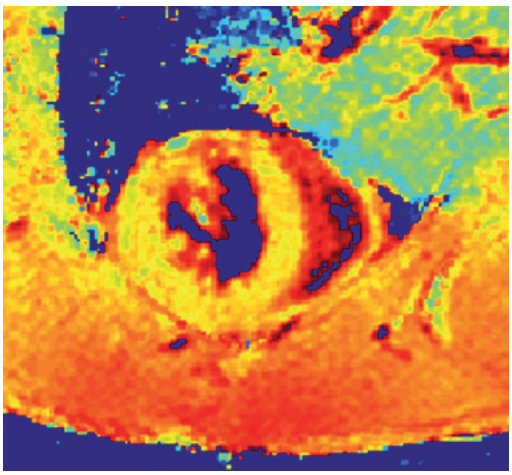

Fig. 9: Myocardial T_1* map of a normal mouse (SAX view).

Outlook

Further improvements in image quality can be achieved using cryogenically cooled RF coil technology for CMR in mice, resulting in a significant sensitivity enhancement over standard room temperature RF-coils. It is important to note, that the enhancement in sensitivity is equivalent to an increase in the magnetic field strength but without the extra challenges – which sometimes can be prohibitive – associated with extreme ultrahigh field MRI.

Summary

As cardiac MR imaging becomes increasingly used for animal research, it should help to advance the capabilities of MRI for the assessment of heart disease. In short, while today's small animal CMR initiatives remain in a state of creative flux, productive engagement in this area continues to drive further developments and helps to harmonize results derived from the preclinical imaging and basic research scenario with that of clinical imaging.

References

[1] Vallee, J.P., et al., *Current status of cardiac MRI in small animals.* MAGMA, 2004. **17** *(3-6): p. 149-56.*

[2] Epstein, F.H., *MR in mouse models of cardiac disease. NMR* Biomed, 2007. **20**(3): p. 238-55.

[3] Ratering, D., et al., *Accelerated cardiovascular magnetic resonance of the mouse heart using self-gated parallel imaging strategies does not compromise accuracy of structural and functional measures.* J Cardiovasc Magn Reson, 2010. **12**: p. 43.

[4] Bovens, S.M., et al., *Evaluation of infarcted murine heart function: comparison of prospectively triggered with self-gated MRI.* NMR Biomed, 2011. **24**(3): p. 307-15

[5] Heijman, E., et al., *Evaluation of manual and automatic segmentation of the mouse heart from CINE MR images.* J Magn Reson Imaging, 2008. **27**(1): p. 86-93.

[6] Young, A.A., et al., *Fast left ventricular mass and volume assessment in mice with three-dimensional guide-point modeling.* J Magn Reson Imaging, 2009. **30**(3): p. 514-20.

[7] Schneider, J.E., et al., *Identification of cardiac malformations in mice lacking Ptdsr using a novel high-throughput magnetic resonance imaging technique.* BMC Dev Biol, 2004. **4**: p. 16.

[8] Li, W., M. Griswold, and X. Yu, *Rapid T_1 mapping of mouse myocardium with saturation recovery Look-Locker method.* Magn Reson Med, 2010. **64**(5): p. 1296-303.

Bruker BioSpin

www.bruker-biospin.com/mri